



CHORUS

This is the accepted manuscript made available via CHORUS. The article has been published as:

Stability and magnetism of strongly correlated single-layer VS_{2}

Houlong L. Zhuang and Richard G. Hennig

Phys. Rev. B **93**, 054429 — Published 26 February 2016

DOI: [10.1103/PhysRevB.93.054429](https://doi.org/10.1103/PhysRevB.93.054429)

Stability and Magnetism of Strongly Correlated Single-Layer VS₂

Houlong L. Zhuang^{1,2} and Richard G. Hennig^{3,2,*}

¹*Department of Mechanical and Aerospace Engineering,
Princeton University, Princeton, New Jersey 08544, U.S.A*

²*Department of Materials Science and Engineering,
Cornell University, Ithaca, New York 14853, U.S.A*

³*Department of Materials Science and Engineering,
University of Florida, Gainesville, Florida 32611, U.S.A*

(Dated: January 15, 2016)

Single-layer transition metal dichalcogenides exhibit a variety of atomic structures and associated exotic electronic and magnetic properties. Density-functional calculations using the LDA+ U approximation show that single-layer VS₂ is a strongly correlated material, where the stability, phonon spectra, and magnetic moments of the octahedral ($1T$) and the trigonal prismatic ($2H$) structures significantly depend on the effective Hubbard U parameter, U_{eff} . Comparison with the HSE06 hybrid density functional used as a benchmark, indicates that $U_{\text{eff}}=2.5$ eV, which consistently shows that the $2H$ structure is more stable than the $1T$ structure and a ferromagnetic semiconductor. The magnetic moments are localized on the V atoms and coupled ferromagnetically due to the superexchange interactions mediated by the S atoms. Calculations of the magnetic anisotropy show an easy-plane for the magnetic moment. Assuming a classical XY model with nearest neighbor coupling, we determine the critical temperature, T_c , for the Berezinsky-Kosterlitz-Thouless transition of $2H$ single-layer VS₂ to be about 90 K. Applying biaxial tensile strains can increase T_c . Using Wannier interpolation, we evaluate the Berry curvature and anomalous Hall conductivity of $2H$ single-layer VS₂. The coexistence of quasi-long range ferromagnetic ordering and semiconducting behavior enables $2H$ single-layer VS₂ to be a promising candidate for spintronics applications.

I. INTRODUCTION

Single-layer transition metal dichalcogenides, MX_2 , have recently become the subject of a great deal of interest owing to a variety of prominent properties.¹ For instance, single-layer MoS₂ exhibits a direct bandgap of 1.9 eV,² which makes it an attractive material for electronics applications.² In contrast to the relatively well explored properties such as electronic,³ optical,^{4,5} and mechanical properties,⁶ magnetism in single-layer MX_2 remains a burgeoning topic.^{7,8} More generally, studying the magnetism in single-layer materials including MX_2 is of fundamental scientific interest and provides guidance for the design of future-generation spintronics devices.⁹⁻¹⁵

Magnetism originates from electron-electron interactions. It has been claimed by Fazekas that “if electron-electron interactions are strong enough to make a system magnetic, then the system is likely to do other remarkable things as well.”¹⁶ We shall see that this claim is true for single-layer vanadium disulfide VS₂, as strong electron correlations lead to ferromagnetic quasi-long range ordering of the spins and affect the energetic and dynamic stability.

Single-layer VS₂ has not yet been successfully synthesized. Nevertheless, there has been intense experimental effort to obtain this single-layer material.¹⁷⁻²⁰ So far, VS₂ nanosheets with the thickness of less than five single layers have been achieved.^{18,20} Similar to a number of other single-layer MX_2 such as MoS₂,²¹ single-layer VS₂ could occur in two common polymorphs, *i.e.* the $1T$ and $2H$ structures that consist of octahedral and trigonal prismatic VS₆ units, respectively. The inset in Fig. 1

illustrates these two structures.

In addition to the experimental work, there have been several density-functional theory (DFT) studies on single-layer VS₂.²²⁻²⁴ Different exchange-correlation functionals were used with the focus on the $1T$, $2H$, or both structures. For example, Ma *et al.* used the generalized gradient approximation (GGA) to investigate the magnetic properties of the metallic $1T$ structure,²⁵ which was assumed to be the stable structure. They observed a non-integer magnetic moment of the system tunable by mechanical strains. Kan *et al.* employed the GGA to study the relative stability of the $1T$ and $2H$ structures, and they found that the $2H$ structure is more stable than the $1T$ structure. The electronic band structures of both structures were further calculated by the GGA+ U ($U_{\text{eff}}=3.0$ eV) and the Heyd-Scuseria-Ernzerhof (HSE06) methods. In a more recent study by Huang *et al.*,²⁶ the HSE06 functional and the GGA+ U ($0 \leq U \leq 4$ eV) method were used to investigate the electronic structures of several single-layer transition metal dichalcogenides. They found that $2H$ single-layer VS₂ is a semiconductor. These previous studies provide valuable perspectives on single-layer VS₂. In our work, we extend these studies by considering the effect of electron correlations and the Hubbard U on several important aspects of the $1T$ and the $2H$ structures, such as their relative stability, phonon spectra, and magnetic moments, and investigate the exchange mechanism that results in the ferromagnetic ordering of the spins in the $2H$ structure.

In this work we perform DFT calculations with the local density approximation (LDA)+ U method to explore the strong correlation effects in single-layer VS₂. We find

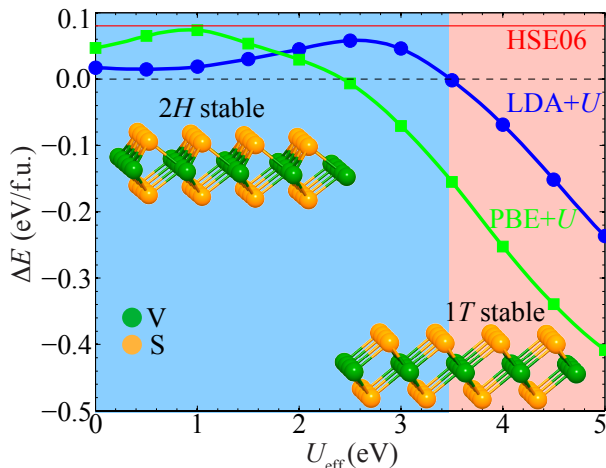


FIG. 1. Energy difference ΔE between $1T$ and $2H$ single-layer VS_2 , $\Delta E = E_{1T} - E_{2H}$, as a function of U_{eff} calculated with the LDA and PBE functionals. The inset illustrates the atomic structures of $1T$ and $2H$ single-layer VS_2 . The red solid line labels the ΔE calculated with the HSE06 functional.

that the effective Hubbard U parameter U_{eff} ranging from 0 to 5 eV drastically affects the stability, phonon spectra, and magnetic moments of single-layer VS_2 . Consistent with the HSE06 results, a value of $U_{\text{eff}} = 2.5$ eV shows that the ferromagnetic semiconducting $2H$ structure is lower in energy than the $1T$ structure, and that both structures exhibit an integer magnetic moment of one Bohr magneton (μ_B). We focus on the more stable $2H$ structure of single-layer VS_2 , which exhibits an interesting coexistence of ferromagnetic ordering and semiconducting properties. We study its electronic structure, and determine that the ferromagnetic order is caused by superexchange interactions. Furthermore, energy calculations including spin-orbit coupling shows isotropic in-plane magnetization, which implies the occurrence of the Berezinsky-Kosterlitz-Thouless transition in $2H$ single-layer VS_2 . We estimate the critical temperature for the transition, T_c , and suggest that mechanical strains can increase T_c . Finally, we compute the Berry curvature and anomalous Hall conductivity. Our work indicates that $2H$ single-layer VS_2 is a potentially useful material for future spintronics devices.

II. METHODS

All DFT calculations are performed using the Vienna *ab initio* simulation package (VASP).^{27,28} The interactions between valence electrons and ionic cores are described with the projector augmented wave (PAW) method.^{29,30} A plane wave basis set with a cutoff energy of 500 eV is used to expand the wavefunctions. For the exchange and correlation, we mainly employ the LDA+ U approximation, and compare with the HSE06^{31,32} and the Perdew-Burke-Ernzerhof (PBE) functionals.³³ The

standard exact-exchange mixing parameter α of 25% is used for the HSE06 functional. We use the LDA PAW potentials for our LDA+ U calculations, and the GGA PAW potentials for the GGA+ U calculations. Atomic configurations including the in-plane lattice constant as well as the atomic positions are fully optimized until the forces are smaller than 0.01 eV/Å. We use a vacuum spacing of 18 Å, which reduces the image interactions caused by the periodic boundary conditions such that the energies are converged to within 1 meV/f.u. and the bandgap to within 1 meV. The Brillouin-zone integration is carried out using $18 \times 18 \times 1$ and $18 \times 18 \times 10$ Monkhorst-Pack k -point meshes for single-layer and bulk VS_2 , respectively. The $3s^23p^63d^34s^2$ states of the V atoms and the $3s^23p^4$ states of the S atoms are treated as valence states. To treat localized V- d orbitals, we use Dudarev's approach with the rotationally invariant effective U parameter $U_{\text{eff}} = U - J$, where U and J are on-site Coulomb and exchange parameters, respectively.³⁴

To study the electronic transport of ferromagnetic single-layer VS_2 , we use the Wannier90 program to calculate the Berry curvature and anomalous Hall conductivity.³⁵

III. RESULTS

First, we determine the ground-state structure of single-layer VS_2 by calculating the energy difference $\Delta E = E_{1T} - E_{2H}$, where E_{1T} and E_{2H} are the energies of the $1T$ and the $2H$ structures, respectively.^{36,37} Figure 1 shows the calculated ΔE using the LDA+ U method with U_{eff} varied from 0 to 5 eV. As can be seen, ΔE is rather sensitive to U_{eff} , suggesting that single-layer VS_2 is a strongly correlated system. Interestingly, we observe a trend that ΔE increases with increasing U_{eff} until it reaches a maximum of 58 meV/f.u. at $U_{\text{eff}} = 2.5$ eV. Beyond this critical U_{eff} , a further increase in U_{eff} leads to smaller ΔE and for $U_{\text{eff}} \geq 3.5$ eV stabilizes the $1T$ structure instead. The trend remains the same if the PBE functional is used, which can be seen in Fig. 1.

Due to the lack of experimental results on single-layer VS_2 , we benchmark our calculated $\Delta E = E_{1T} - E_{2H}$ with the result from the HSE06 functional, which provides an alternative description for strongly correlated systems.³⁸ The HSE06 functional predicts that the $2H$ structure is the ground-state for single-layer VS_2 , with a ΔE of 80 meV/f.u.³⁹ This motivates our choice of $U_{\text{eff}} = 2.5$ eV within the LDA+ U formalism, which provides good agreement with the hybrid density functional result.

The U_{eff} parameter affects not only the energy difference as described above, but also the magnetic moments. Figure 2 shows the calculated total magnetic moment per unit cell of $1T$ and $2H$ single-layer VS_2 with the LDA+ U method, where U_{eff} is changed from 0 to 5 eV. We observe that the magnetic moment for both structures increases with U_{eff} and saturates to a value of 1.0 μ_B . This is because increasing U_{eff} enhances the electron local-

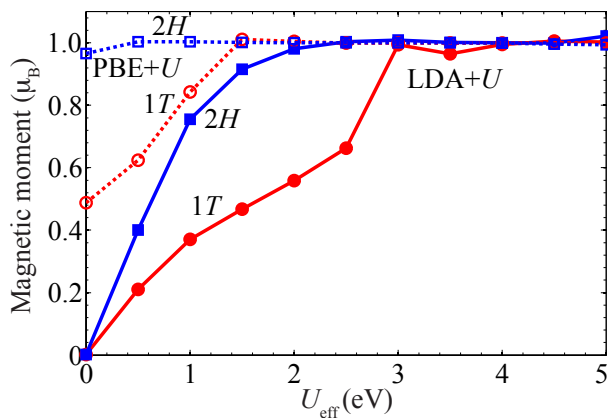


FIG. 2. Magnetic moment of 1T and 2H single-layer VS₂ per formula unit calculated with the LDA + U (solid lines) and PBE + U (dotted lines) methods, where U_{eff} is varied from 0 to 5 eV.

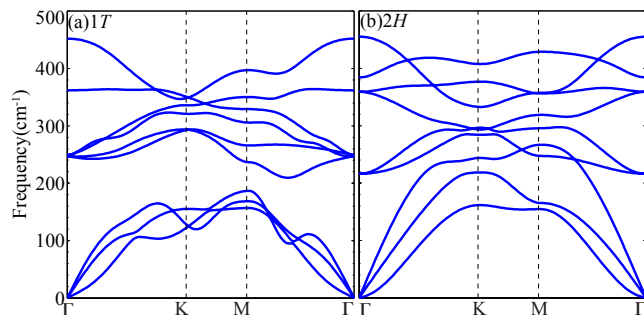


FIG. 3. Calculated phonon spectra of (a) 1T and (b) 2H single-layer VS₂ with the LDA+ U ($U_{\text{eff}} = 2.5$ eV) method.

ization and opens a bandgap in single-layer VS₂. The PBE+ U method leads to a similar trend as also seen in Fig. 2. Consistent again with the LDA + U ($U_{\text{eff}} = 2.5$ eV) method, the HSE06 functional shows that both the 1T and the 2H structures exhibit a magnetic moment of $1.0 \mu_{\text{B}}$. Common to the three methods – LDA+ U , PBE+ U , and HSE06, we observe that the magnetic moment is strongly localized on the V ions, which indicates that d electrons in a V ion in single-layer VS₂ adopt the d^1 configuration.

In view of the above discussion, we emphasize the importance of either including the U_{eff} parameter to the LDA or PBE functional or to employ a hybrid functional such as HSE06 for the calculation of the magnetic structure of single-layer VS₂. Without using U_{eff} , the LDA functional predicts a negligible magnetic moments for both the 1T and 2H structures, while the PBE functional results in an inaccurate fractional magnetic moments as previously reported.^{22,25} Including a Hubbard U results in good agreement with hybrid density functionals and predicts ferromagnetic ordering in the 1T or 2H single-layer VS₂.

To evaluate the feasibility of isolating 2H single-layer VS₂ from bulk VS₂, we calculate the formation energy,

TABLE I. Comparison of the structure predictions with the LDA+ U ($U_{\text{eff}} = 2.5$ eV) method and the HSE06 functional. In-plane lattice constant a in Å, V-S-V bond angle θ in degrees, magnetic moment per unit cell m_s in μ_{B} , spin-up $E_{g\uparrow}$ and spin-down $E_{g\downarrow}$ bandgaps of 2H single-layer VS₂. The energy difference between the 1T and 2H structure is denoted as ΔE_f and ΔE_{mag} is the energy difference between the FM and AFM state of 2H single-layer VS₂ for the relaxed FM structure. Both energy differences are in units of meV per formula unit.

Methods	a	θ	m_s	$E_{g\uparrow}$	$E_{g\downarrow}$	ΔE_f	ΔE_{mag}
LDA+ U	3.12	83.86	1.00	0.87	0.85	58	70
HSE06	3.15	84.61	1.00	1.14	1.96	80	158

TABLE II. Formation energy (in meV/atom) of 2H single-layer VS₂ calculated with various methods including the LDA, LDA+ U ($U_{\text{eff}} = 2.5$ eV), PBE, PBE+ U ($U_{\text{eff}} = 1.0$ eV), vdW-DF-optB88, and vdW-DF-optB88+ U ($U_{\text{eff}} = 1.0$ eV).

	LDA	LDA+ U	PBE	PBE+ U	vdW	vdW+ U
E_f	55.0	33.8	-13.4	-21.7	75.2	67.9

ΔE_f , defined as the energy difference between single-layer and bulk VS₂ with the CdI₂-type structure. Table II summarizes the calculated ΔE_f with various methods. We observe that the LDA, LDA+ U ($U_{\text{eff}} = 2.5$ eV), van der Waals (vdW)-DF-optB88,^{40–42} and vdW+ U ($U_{\text{eff}} = 1.0$ eV) methods predict a similar formation energy that is comparable to other single-layer materials such as MoS₂ that have been successfully isolated from their bulk counterparts with layered structures.³⁷ In contrast, the PBE and the PBE+ U ($U_{\text{eff}} = 1.0$ eV) methods lead to unphysical negative formation energies due to the underestimate of interlayer binding energy in bulk VS₂. The small ΔE_f of 2H single-layer VS₂ indicates that it could be obtained by mechanical exfoliation.

Both the 1T and 2H structure are dynamically stable, which can be seen from their phonon spectra displayed in Fig. 3. However, since the 2H structure is lower in energy than the 1T one, we henceforth characterize the structural, electric, magnetic, and electrical transport properties of this stable structure using the LDA+ U ($U_{\text{eff}} = 2.5$ eV) method. Table I summarizes the in-plane lattice constant and the V-S-V bond angle of 2H single-layer VS₂. In addition, we examine the energy difference ΔE_{mag} between the ferromagnetic (FM) and antiferromagnetic (AFM) configurations using a 2×2 supercell. We find that the FM state is 94 meV/f.u. lower than the AFM one, which shows that 2H single-layer VS₂ indeed exhibits ferromagnetism. All of these results agree reasonably well with the ones using the HSE06 functional.

In addition to exhibiting ferromagnetism, 2H single-layer VS₂ is a semiconductor. The electronic band structures displayed in Fig. 4 shows a direct bandgap in the spin-up channel and an indirect one in the spin-down

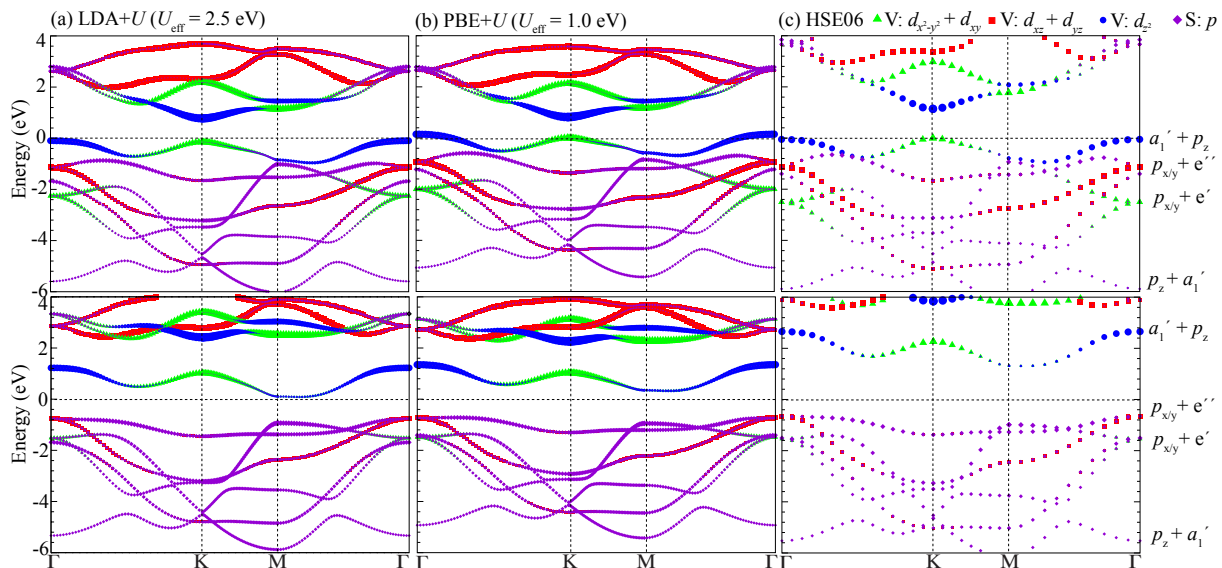


FIG. 4. Orbital resolved (top) spin-up and (bottom) spin-down band structures of $2H$ single-layer VS_2 calculated with the (a) LDA+ U ($U_{\text{eff}} = 2.5$ eV), (b) PBE+ U ($U_{\text{eff}} = 1.0$ eV), and (c) HSE06 methods. (c) Electron density corresponding to the valence band maximum states in the spin-up band structure illustrating the $d_{z^2}(a'_1)$ character. The isosurface value is set to $0.01 e/a_0^3$, where a_0 is the Bohr radius.

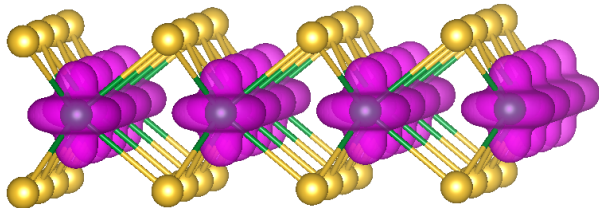


FIG. 5. Electron density corresponding to the valence band maximum states in the spin-up band structure illustrating the $d_{z^2}(a'_1)$ character. The isosurface value is set to $0.01 e/a_0^3$, where a_0 is the Bohr radius.

channel. Table I compares the LDA+ U bandgaps with our HSE06 calculations, which agree well with a recent theoretical study using the same functional.²⁶ Comparing to the LDA+ U ($U_{\text{eff}} = 2.5$ eV) bandgaps, the HSE06 functional predicts somewhat larger bandgaps, particularly for the spin-down channel. However, confirmation of the bandgaps still awaits experimental measurements. More importantly, the rare coexistence of ferromagnetism and semiconducting in $2H$ single-layer VS_2 ensures it to be useful for spintronics applications.

Ferromagnetism is a co-operative phenomenon that arises from the exchange interactions among electrons.⁴³ To understand the mechanism of the exchange coupling in $2H$ single-layer VS_2 that results in the ferromagnetic ordering, we calculate the orbital-resolved spin-up and spin-down band structures, which are displayed in Figs. 4(a). The PBE and HSE06 band structures in Figs. 4(b) and (c) exhibit qualitatively the same features. The crystal-field splitting associated with the D_{3h} sym-

metry of $2H$ single-layer VS_2 splits the degeneracy of the atomic d -orbitals of the V atoms. For an isolated VS_6 complex, the splitting results in three groups of orbitals, e' ($d_{x^2-y^2}$ and d_{xy} orbitals), e'' (d_{xz} and d_{yz} orbitals), and a'_1 (d_{z^2} orbital). Figs. 4(a) shows that the states at the Γ point display this splitting with the energy of the orbitals decreasing from e' to e'' to a'_1 .

Based on the orbital analysis and in agreement with the electronegativities of V (1.63) and S (2.58) atoms by the Pauling scale,⁴⁴ $2H$ single-layer VS_2 exhibits covalent bonds with small ionic character of about 20%. The e' and e'' d orbitals strongly hybridize with the S p_x and p_y orbitals and form bands of bonding and antibonding states. The bonding states are occupied and the antibonding ones are empty. Due to its symmetry and the symmetry of the structure, the a'_1 (d_{z^2}) orbital cannot hybridize with the S p_x and p_y orbital and has limited overlap with the S p_z orbitals. It hybridizes with the S p_z orbital forming bands of bonding and antibonding states. The bonding states show mostly S p_z character and are doubly occupied. The antibonding states show mostly V a'_1 character and are split by the Hubbard U interaction into an up and down spin band. The up-spin band is located at the valence band maximum. Hence, the magnetic states in VS_2 come from the singly occupied a'_1 orbital on the V atoms.

The top valence band in Fig. 4(a) shows that one spin-up electron is localized in the d band with mixed $d_{x^2-y^2}$, d_{xy} , and d_{z^2} orbital character. The corresponding electron density isosurface illustrated in Fig. 5 matches well the shapes of these orbitals. Furthermore, we observe little overlap of these d orbitals between V ions, implying that the direct exchange mechanism is unlikely. In-

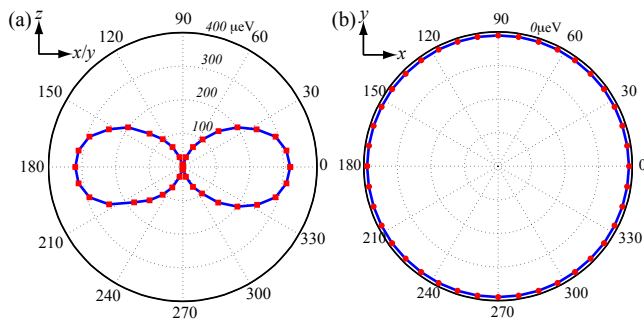


FIG. 6. Angular dependence of MAE of $2H$ single-layer VS_2 with the direction of magnetization lying (a) on the xz or yz plane and (b) on the xy plane. The MAE is calculated with reference to the energy minimum when the magnetization locates on the xy plane. We observe an easy plane for the spin oriented within the plane of the 2D material.

stead, the more probable exchange mechanism is a superexchange interaction between the V atoms mediated by the neighboring S atoms. According to Kahn *et al.*,⁴⁵ the exchange integral J has the following approximate relation,⁴⁶

$$J \approx 2k - 4\beta S. \quad (1)$$

The first term is called the potential exchange, which is positive favoring ferromagnetism due to Hund's first rule.⁴⁷ The second term is named the kinetic exchange and favors antiferromagnetism. It consists of the hopping integral β and the overlap integral S . As shown in Tab. I, the V-S-V angle is close to 90° , which means that the S p orbitals are nearly orthogonal to the V d orbitals, leading to a negligible overlap integral. This is also in line with the Goodenough-Kanamori rules,^{48–50} *i.e.* the super-exchange of an orthogonal configuration is dominated by the ferromagnetic contribution. As a result, $2H$ single-layer VS_2 adopts a ferromagnetic ordered ground state.

We proceed to evaluate the critical temperature of the ferromagnetic transition in $2H$ single-layer VS_2 . The Mermin-Wagner theorem proves that continuous symmetries cannot be spontaneously broken at finite temperatures by short-range interactions in a 2D material.⁵¹ However, there are two models that can show magnetic ordering in a 2D material, the 2D Ising model and the XY model. In the Ising model, the symmetry is discrete and corresponds to a magnetic system where the spins exhibit a preferred axis. In this case, the 2D material displays a second order phase transition to a magnetically ordered phase.⁵² The XY model corresponds to a 2D material where the magnetization exhibits an easy plane. For this case, the material shows a quasi-long range ordered phase at low temperatures with a power-law decay of the correlation function.⁵³ Therefore, whether a 2D material exhibits a magnetically ordered phase depends on the magnetocrystalline anisotropy energy (MAE) and the distance dependence of the exchange interaction.

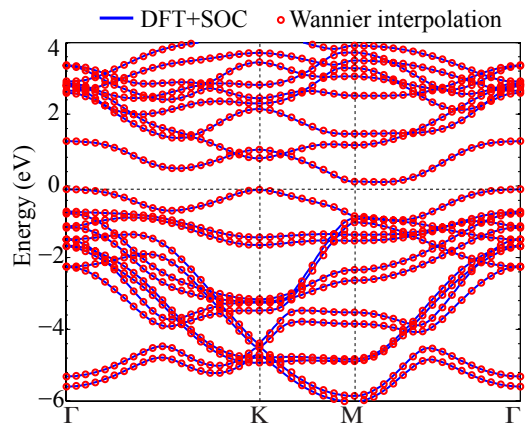


FIG. 7. Comparison of the band structures obtained from the DFT+SOC calculation and the Wannier interpolation.

To determine the MAE of $2H$ single-layer VS_2 , we first calculate the total energies of the material with the spin of V atom constrained in different directions on the xz , yz , and xy planes. The spin-orbit coupling is included in all the energy calculations. Then the MAE are defined as the energy differences with reference to the energy-minimum spin configuration on each plane. Fig. 6 illustrates the MAE as a function of polar angles on the xz , yz , and xy planes. We observe a strong dependence of the MAE on the out-of-plane angle of the magnetic moment, and an easy xy plane. This implies that $2H$ single-layer VS_2 belongs to the category of XY magnets. Namely, the so-called Berezinsky-Kosterlitz-Thouless transition could occur at the critical temperature T_c , which can be calculated as $T_c = 0.89J/k_B$,⁵⁴ where J is the exchange integral between adjacent spins and k_B is the Boltzmann constant. The exchange integral is straightforwardly calculated from the ΔE_{mag} listed in Tab. I, *i.e.* $\Delta E_{\text{mag}} = 8J$. We obtain for the nearest-neighbor exchange interaction $J = 8.7$ meV with the LDA+ U method and predict a T_c of around 90 K. Although this temperature is below room temperature, it is comparable to the calculated T_c of several other predicted single-layer magnetic materials such as MnO_2 (140 K)⁹ and manganese phthalocyanine (~ 150 K).¹¹

A common strategy to increase T_c is to apply mechanical strains.¹³ We find that a biaxial tensile strain of 5% increases J to 11.1 meV, corresponding to an increase in T_c to 115 K. The increased J reflects the enhanced superexchange interaction due to the increased V-S-V angle from 83.9° to 86.9° that is closer to the ideal 90° , which minimizes the overlap integral S in Eq. 1.

Finally, we study the electronic transport properties of $2H$ single-layer VS_2 . As expected, the ferromagnetic ordering gives rise to an anomalous Hall conductivity (AHC). We calculate the AHC, which is the integral of the Berry curvature $\Omega_z(k)$ in the first Brillouin zone

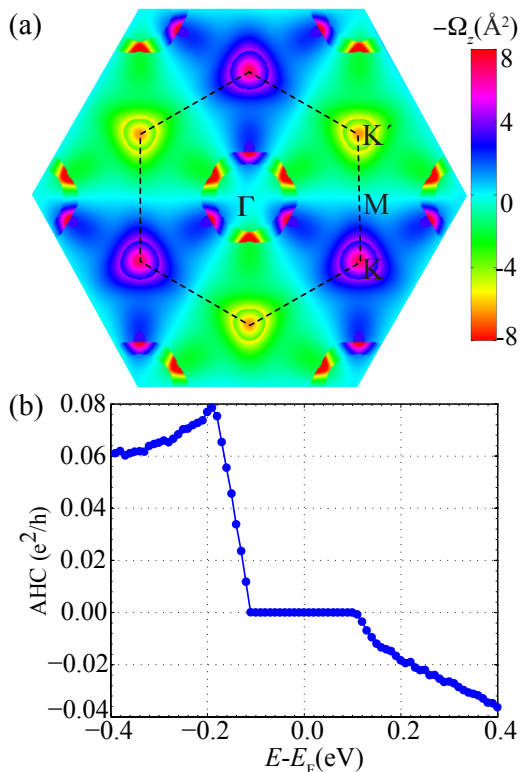


FIG. 8. (a) Berry curvature and (b) anomalous Hall conductivity of $2H$ single-layer VS_2 .

(BZ),^{55–57}

$$\sigma_{xy} = -\frac{e^2}{\hbar} \int_{BZ} \Omega_z(k) dk. \quad (2)$$

We use Wannier interpolation and construct 22 Wannier orbitals from the V d and S p orbitals from a self-consistent calculation including spin-orbit coupling (SOC). The excellent agreement between the DFT+SOC and Wannier interpolated band structures is shown in Fig. 7. Fig. 8(a) shows the calculated Berry curvature $\Omega_z(k)$ using a 400×400 k -point mesh. Similar to the Berry curvature of $2H$ single-layer MoS_2 ,⁵⁸ we observe different signs of $\Omega_z(k)$ at the K and K' points due to the lack of inversion symmetry in $2H$ single-layer VS_2 .

Fig. 8(b) depicts the AHC as a function of the Fermi level, which can be controlled through doping. We predict a non-zero AHC over a wide energy range. However, the AHC curve displays no quantized Hall plateaus, in-

dicating that $2H$ single-layer VS_2 is not a Chern insulator due to the weak SOC. Indeed, we calculate the orbital magnetic moment of V ions, which is merely $0.012 \mu_B$ showing that the orbital angular momentum is almost completely quenched. One possible method to obtain a VS_2 -based Chern insulator may be doping $2H$ single-layer VS_2 with heavy atoms to increase the SOC strength.⁵⁹

IV. CONCLUSIONS

We determined the structural stability and electronic and magnetic properties of single-layer VS_2 using the density-functional theory with the LDA+ U and HSE06 exchange-correlation functionals. We investigated two possible polymorphs, *i.e.* the octahedral $1T$ and the trigonal prismatic $2H$ structure. We showed that single-layer VS_2 exhibits strong correlation effects, which are reflected by the strong dependence of stability and magnetic moments of the two structures on the effective Hubbard U parameter. Both the LDA+ U ($U_{\text{eff}} = 2.5$ eV) method and the HSE06 functional reveals that the $2H$ structure is the ground state structure with ferromagnetic ordering and semiconducting properties. We suggest that superexchange is the mechanism that leads to the ferromagnetism in $2H$ single-layer VS_2 . In addition, we find that $2H$ single-layer VS_2 displays opposite Berry curvature at the K and K' points, and an anomalous Hall conductivity dependent on doping energy levels. Experiments of synthesizing single-layer VS_2 and characterizing its electronic and magnetic properties are called for to confirm our findings. Two interesting questions arise from our work: (i) What is the phase transition mechanism from the $1T$ to the $2H$ structure? (ii) Is there any other possible structure that is more stable than the $1T$ and the $2H$ ones? These questions are the subjects of our future work.

ACKNOWLEDGMENTS

This work was supported by the NSF under the CAREER award No. DMR-1056587 and under award No. ACI-1440547. This research used computational resources of the Texas Advanced Computing Center under Contracts No. TG-DMR050028N and No. TG-DMR140067. We also thank Dr. Richard Evans, Dr. Satoshi Okamoto, and Prof. Robert B. Van Dover for helpful discussions.

* rhennig@ufl.edu

¹ Q. H. Wang, K.-Z. Kouros, A. Andras, J. N. Coleman, and M. S. Strano, *Nature Nanotech.* **7**, 699 (2012).

² K. F. Mak, C. Lee, J. Hone, J. Shan, and T. F. Heinz, *Phys. Rev. Lett.* **105**, 136805 (2010).

³ D. Xiao, G.-B. Liu, W. Feng, X. Xu, and W. Yao, *Phys. Rev. Lett.* **108**, 196802 (2012).

⁴ K. F. Mak, K. He, C. Lee, G. H. Lee, J. Hone, T. F. Heinz, and J. Shan, *Nature Mater.* **12**, 207 (2013).

⁵ C.-Y. Wang and G.-Y. Guo, *The Journal of Physical Chemistry C* **119**, 13268 (2015).

- ⁶ S. Bertolazzi, J. Brivio, and A. Kis, *ACS Nano* **5**, 9703 (2011).
- ⁷ Z. Zhang, X. Zou, V. H. Crespi, and B. I. Yakobson, *ACS Nano* **7**, 10475 (2013).
- ⁸ S. Tongay, S. S. Varnoosfaderani, B. R. Appleton, J. Wu, and A. F. Hebard, *Applied Physics Letters* **101**, 123105 (2012).
- ⁹ M. Kan, J. Zhou, Q. Sun, Y. Kawazoe, and P. Jena, *The Journal of Physical Chemistry Letters* **4**, 3382 (2013).
- ¹⁰ M. Kan, S. Adhikari, and Q. Sun, *Phys. Chem. Chem. Phys.* **16**, 4990 (2014).
- ¹¹ J. Zhou and Q. Sun, *Journal of the American Chemical Society* **133**, 15113 (2011).
- ¹² X. Li and J. Yang, *J. Mater. Chem. C* **2**, 7071 (2014).
- ¹³ M. Kan, S. Adhikari, and Q. Sun, *Phys. Chem. Chem. Phys.* **16**, 4990 (2014).
- ¹⁴ Y. Zhou, Z. Wang, P. Yang, X. Zu, L. Yang, X. Sun, and F. Gao, *ACS Nano* **6**, 9727 (2012).
- ¹⁵ S. Zhang, Y. Li, T. Zhao, and Q. Wang, *Sci. Rep.* **4**, 5241 (2014).
- ¹⁶ P. Fazekas, *Lecture Notes on Electron Correlation and Magnetism* (World Scientific Pub Co Inc, 1999).
- ¹⁷ C. S. Rout, B.-H. Kim, X. Xu, J. Yang, H. Y. Jeong, D. Odhkuu, N. Park, J. Cho, and H. S. Shin, *Journal of the American Chemical Society* **135**, 8720 (2013).
- ¹⁸ J. Feng, X. Sun, C. Wu, L. Peng, C. Lin, S. Hu, J. Yang, and Y. Xie, *Journal of the American Chemical Society* **133**, 17832 (2011).
- ¹⁹ C. Song, K. Yu, H. Yin, H. Fu, Z. Zhang, N. Zhang, and Z. Zhu, *J. Mater. Chem. C* **2**, 4196 (2014).
- ²⁰ D. Gao, Q. Xue, X. Mao, W. Wang, Q. Xu, and D. Xue, *J. Mater. Chem. C* **1**, 5909 (2013).
- ²¹ Y.-C. Lin, D. O. Dumcenco, Y.-S. Huang, and K. Suenaga, *Nature Nanotech.* **9**, 391396 (2014).
- ²² L.-Y. Gan, Q. Zhang, Y. Cheng, and U. Schwingenschlögl, *Phys. Rev. B* **88**, 235310 (2013).
- ²³ A. H. M. Abdul Wasey, S. Chakrabarty, and G. P. Das, *Journal of Applied Physics* **117**, 064313 (2015).
- ²⁴ M. Kan, B. Wang, Y. Lee, and Q. Sun, *Nano Research* , 1 (2014).
- ²⁵ Y. Ma, Y. Dai, M. Guo, C. Niu, Y. Zhu, and B. Huang, *ACS Nano* **6**, 1695 (2012).
- ²⁶ P.-R. Huang, Y. He, H. K. Pal, and M. Kindermann, *ArXiv e-prints* (2015), arXiv:1501.00760.
- ²⁷ G. Kresse and J. Hafner, *Phys. Rev. B* **47**, 558 (1993).
- ²⁸ G. Kresse and J. Furthmüller, *Phys. Rev. B* **54**, 11169 (1996).
- ²⁹ P. E. Blöchl, *Phys. Rev. B* **50**, 17953 (1994).
- ³⁰ G. Kresse and D. Joubert, *Phys. Rev. B* **59**, 1758 (1999).
- ³¹ J. Heyd, G. E. Scuseria, and M. Ernzerhof, *The Journal of Chemical Physics* **118**, 8207 (2003).
- ³² J. Heyd, G. E. Scuseria, and M. Ernzerhof, *The Journal of Chemical Physics* **124**, 219906 (2006).
- ³³ J. P. Perdew, K. Burke, and M. Ernzerhof, *Phys. Rev. Lett.* **77**, 3865 (1996).
- ³⁴ S. L. Dudarev, G. A. Botton, S. Y. Savrasov, C. J. Humphreys, and A. P. Sutton, *Phys. Rev. B* **57**, 1505 (1998).
- ³⁵ N. Marzari, A. A. Mostofi, J. R. Yates, I. Souza, and D. Vanderbilt, *Rev. Mod. Phys.* **84**, 1419 (2012).
- ³⁶ H. L. Zhuang and R. G. Hennig, *Applied Physics Letters* **101**, 153109 (2012).
- ³⁷ H. L. Zhuang and R. G. Hennig, *Journal of The Minerals, Metals & Materials Society (TMS)* **66**, 366 (2014).
- ³⁸ G. Gou, I. Grinberg, A. M. Rappe, and J. M. Rondinelli, *Phys. Rev. B* **84**, 144101 (2011).
- ³⁹ Increasing the fraction of exact exchange from 0 to 0.5 changes the sign of ΔE around $\alpha = 0.32$.
- ⁴⁰ G. Román-Pérez and J. M. Soler, *Phys. Rev. Lett.* **103**, 096102 (2009).
- ⁴¹ T. Thonhauser, V. R. Cooper, S. Li, A. Puzder, P. Hyldgaard, and D. C. Langreth, *Phys. Rev. B* **76**, 125112 (2007).
- ⁴² M. Dion, H. Rydberg, E. Schröder, D. C. Langreth, and B. I. Lundqvist, *Phys. Rev. Lett.* **92**, 246401 (2004).
- ⁴³ D. Wagner, *introduction to the Theory of Magnetism* (Pergamon Press; 1st edition, 1973).
- ⁴⁴ L. Pauling, *The nature of the chemical bond and the structure of molecules and crystals* (Cornell University Press, 1960).
- ⁴⁵ J. J. Girerd, Y. Journaux, and O. Kahn, *Chemical Physics Letters* **82**, 534 (1981).
- ⁴⁶ J.-P. Launay and M. Verdaguer, *Electrons in Molecules: From Basic Principles to Molecular Electronics* (Oxford University Press; 1st edition, 2013).
- ⁴⁷ P. A. Cox, *Transition metal oxides: an introduction to their electronic structure and properties* (Oxford University Press, New York, 2010).
- ⁴⁸ J. B. Goodenough, *Phys. Rev.* **100**, 564 (1955).
- ⁴⁹ G. Blasse, *Journal of Physics and Chemistry of Solids* **26**, 1969 (1965).
- ⁵⁰ J. Kanamori, *Journal of Physics and Chemistry of Solids* **10**, 87 (1959).
- ⁵¹ N. D. Mermin and H. Wagner, *Phys. Rev. Lett.* **17**, 1133 (1966).
- ⁵² C. N. Yang, *Phys. Rev.* **85**, 808 (1952).
- ⁵³ J. V. Jose, *40 years of Berezinskii-Kosterlitz-Thouless theory* (World Scientific Publishing Company, 2013).
- ⁵⁴ J. F. Fernández, M. F. Ferreira, and J. Stankiewicz, *Phys. Rev. B* **34**, 292 (1986).
- ⁵⁵ X. Wang, J. R. Yates, I. Souza, and D. Vanderbilt, *Phys. Rev. B* **74**, 195118 (2006).
- ⁵⁶ W. Feng, Y. Yao, W. Zhu, J. Zhou, W. Yao, and D. Xiao, *Phys. Rev. B* **86**, 165108 (2012).
- ⁵⁷ Y. Yao, L. Kleinman, A. H. MacDonald, J. Sinova, T. Jungwirth, D.-s. Wang, E. Wang, and Q. Niu, *Phys. Rev. Lett.* **92**, 037204 (2004).
- ⁵⁸ T. Cao, G. Wang, W. Han, H. Ye, C. Zhu, J. Shi, Q. Niu, P. Tan, E. Wang, B. Liu, and J. Feng, *Nature Commun.* **3**, 887 (2012).
- ⁵⁹ K. F. Garrity and D. Vanderbilt, *Phys. Rev. Lett.* **110**, 116802 (2013).